Sub-T_g Relaxation Behavior of Corona-Poled Nonlinear Optical Polymer Films and Views on Physical Aging

Geoffrey A. Lindsay,* Ronald A. Henry, and James M. Hoover

Chemistry Division, Research Department, Naval Air Warfare Center Weapons Division, China Lake, California 93555

Andre Knoesen

Electrical Engineering & Computer Science Department, University of California, Davis, California 95616

Mohammad A. Mortazavi

Advanced Technology Group, Hoechst Celanese Corporation, 86 Morris Avenue, Summit, New Jersey 07901

ABSTRACT: The complete synthesis and characterization of a poly(methyl methacrylate-*co*-coumaromethacrylate) is described. Thin films of this polymer were corona-poled and aged under various conditions. The intensity of second harmonic light, generated by passing a laser beam through the polarized films, indicated the average degree of dipole alignment in the films as a function of time and temperature. The long-term aging data were fit with biexponential and stretched exponential equations. A model based on diffusion of defects (holes) in a locally heterogeneous glassy matrix is discussed.

Introduction

Recently, there has been immense interest in second-order nonlinear optical polymer (NLOP) films[1] because of their large nonlinear optical coefficients and their high electrooptic switching speed (10's of GHz). NLOP can be spin-cast and processed into optical waveguides by using conventional microlithiography. These new polymers are under development for application in electrooptical modulators,[2] switches,[3] and optical interconnects.[4] Understandably, the ability to predict and control the molecular relaxation processes in these polymers for improving optical stability and longevity is of tremendous technological importance.

A useful process for the fabrication of a second-order NLOP film is electric field poling.[5] A glassy polymer containing chromophores (i.e., dyes) that have large second-order susceptibility[1a] is heated and poled near the glass transition temperature (T_g), then cooled below the T_g while still applying the electric field. After the external field is removed, a net alignment of dipole moments can remain essentially locked in the film for years, as long as the temperature of the film remains well below the T_g.

The polarizability of the chromophores and their noncentrosymmetric arrangement in the polymer film enable the generation of light at the second harmonic (SH) frequency when a laser beam is transmitted through the film.[6] Several investigators have shown that monitoring the change of the SH signal intensity in poled films offers a new analytical tool for investigating molecular motions near and below the glass transition temperature.[7]

Several studies on the relaxation of order in poled polymer films have been carried out on solid solutions in which a dye containing a large dipole moment was dissolved in an amorphous, glassy polymer, such as polystyrene or poly(methyl methacrylate).[8] In these so-called guest-host systems, often the thermodynamic solubility of the dye in the polymer is limited; therefore, one must consider the tendency of the dye to form small aggregates upon aging. Furthermore, the dye is decoupled to some extent from the backbone of the polymer.

In the present paper we have investigated the relaxation of chromophores chemically attached as side chains in a well-characterized, high molecular weight, amorphous copolymer containing about one side chain per four backbone repeat units. We compare various relaxation models with the data, and elaborate on a model involving diffusion of holes in a heterogeneous glassy matrix. In an earlier paper, we reported the linear electrooptic coefficient as a function of wavelength of the same polymer reported here.[9]

Experimental Section

We have been developing new comb-shaped polymers that contain coumarin sidechains.[10] This paper gives the first detailed description of the synthetic procedure for preparing a coumaromethacrylate copolymer. The structure is shown in Figure 1.

Coumarin Monomer Synthesis. The hydroxy-functional precursor, *N*-(2-hydroxyethyl)-7-(diethylamino)coumarin-3-carboxamide (HFC), was prepared in two steps. First, 4-(diethylamino)salicylaldehyde was reacted with an equal molar amount of dimethyl malonate in methanol (piperidine catalyst) at room temperature overnight. The solvent was removed on a rotary evaporator at room temperature, and the remaining oil was chromatographically purified by dissolving it in chloroform and passing the solution through a silica column. A 61% yield of 3-carbomethoxy-7-(diethylamino)coumarin (CMDEAC) was recovered from the unreacted starting materials. Second, a mixture of the CMDEAC oil and ethanolamine was refluxed in benzene for 24 h. Gummy crystals formed upon cooling. After washing with cold benzene and recrystallizing from benzene, a 25% yield of HFC, melting at 126-127 °C, was obtained. (Elemental analysis indicated 63.9% C, 6.67% H, and 8.87% N; theoretical is 63.1% C, 6.62% H, and 9.21% N.)

The polymerizable methacrylate ester of HFC (CMA) was prepared by coupling equal molar amounts of HFC and methacrylic acid in methylene chloride solution with dicyclohexylcarbodiimide at room temperature (in the presence of 4-(diethylamino)pyridine catalyst and 4-methoxyphenol stabilizer). Dicyclohexylurea precipitate was filtered off. The remaining solution was evaporated, and the dark yellow solid was dissolved in a benzene/cyclohexane mixture. This solution was stirred with Celite, filtered, and diluted with *n*-hexane. The turbid solution slowly deposited yellow crystals during several days at
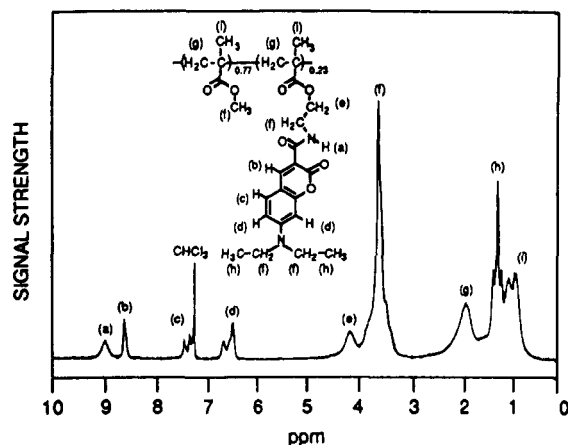
Figure 1. 80-MHz proton magnetic resonance and structure of polymer 1295-6.

Figure 2. Differential thermal analysis

Figure 3. Dielectric analysis (DEA).

room temperature. The CMA product was a coarse yellow crystalline solid that melted at 143-144 °C. Proton nuclear magnetic resonance (^{1}H NMR) and elemental analysis were consistent with the desired product. (Elemental analysis indicated 64.7% C, 6.75% H, and 7.24% N; theoretical is 64.5% C, 6.5% H, and 7.52% N.)

Polymer Synthesis. The poly(methyl methacrylate-*co*-coumaromethacrylate) was synthesized by free radical polymerization of methyl methacrylate and CMA in chlorobenzene. The polymer was precipitated into a large excess of methanol, filtered, dried 2 h under vacuum at 100 °C, then ground to a powder, and dried overnight near the glass transition temperature. Thermal gravimetric analysis of the powder showed that less than 1% volatiles remained in the polymer. The same batch of polymer was redissolved in chlorobenzene to make the films used for all of the optical measurements in this paper.

Characterization. The concentration of coumarin groups in this polymer was about 1.0×10^{21} molecules per cubic centimeter, which corresponds to about 23 mol % of the monomer units by ^{1}H NMR. The chemical structure and ^{1}H NMR spectrum are shown in Figure 1. Proton assignments (ppm) are as follows: (a) 8.99 amide; (b) 8.63 coumaro vinylic; (c) 7.45, 7.34, 7.29 and (d) 6.65, 6.48 coumaro aromatic; (e) 4.07 and (f) 3.54 (and shoulder region) nonbackbone methylene and ester methyl; (g) 1.85 backbone methylene; (h) 1.20 (triplet) ethyl amino methyl; and (i) 0.97, 0.83 acrylic α-methyl. The coumarin group's dipole moment was estimated to be about 5 D.[11]

The weight-average molecular weight of this polymer was 101 000 g/mol (vs polystyrene standards) by gel permeation chromatography (GPC) in chloroform solution. GPC preparative Styragel columns of 500 and 10 000 Å were used. The polydispersity of molecular weights, M_w/M_n, was 2.05. The GPC curve had a monomodal, Gaussian distribution.

The glass transition temperature of the polymer used for this study was about 135 °C, the midpoint of the transition by differential scanning calorimetry (second heating scan) as shown in Figure 2. There were no signs of a crystalline endotherm between -20 and 220 °C. A TA Instrument DSC 2910 was used for the thermal analysis.

The dielectric relaxation scans are shown in Figure 3. A TA Instrument DEA 2970 was used. Films for the dielectric measurements were prepared by heating and pressing polymer powder on the DEA sensor. The dielectric constant of the polymer reported in Figure 3 was low due to voids remaining in the polymer film; however, changes in dielectric constant with temperature were reproducible. In addition to the T_g, a β transition (T_β) is apparent at about 52 °C in the 0.1-Hz scan, but not at higher frequencies. The molecular motions above 150 °C will not be discussed in this paper.

Film Preparation for Optical Measurements. Polymer films were prepared by the spin-cast or blade-cast techniques from chlorobenzene solutions. Solutions were cast on glass microscope slides (BK-7 silica) and baked in vacuum (0.5 mmHg) for 12 h at 150 °C. The importance of removing the last traces of solvent from the films cannot be overstated.[12] Thicknesses
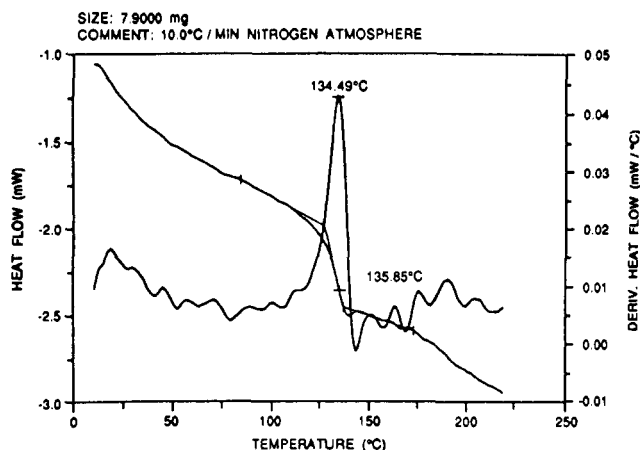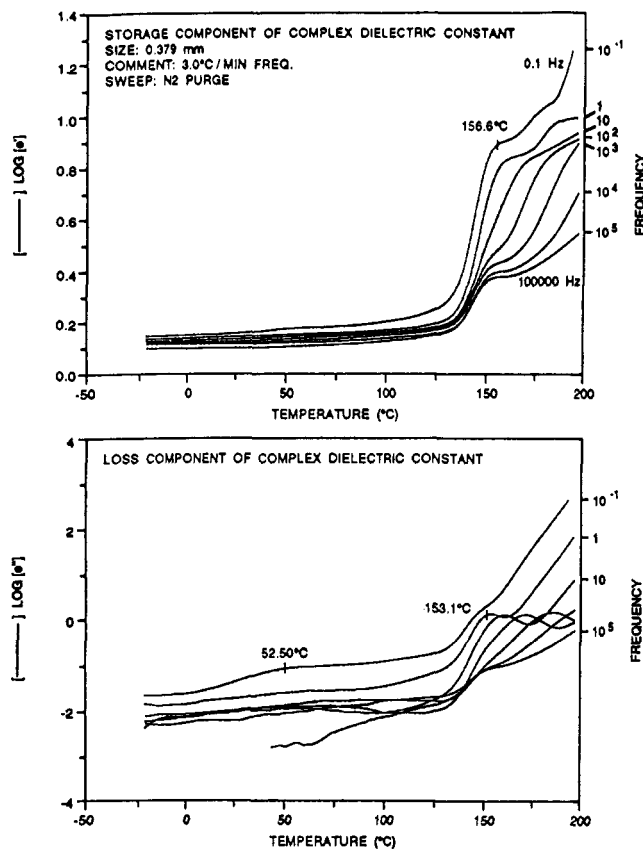
ranged from 0.5 to 2.0 μm for spin-cast films and 2.0 to 5.0 μm for blade-cast films, as measured by a Dektak 3030 stylus profilometer.

Poling. These thin films of the polymer were poled for 5 min at 150 °C at corona onset (1-2 μA at 5000 V) in air with a positively charged, parallel wire 1 cm above the exposed NLOP film. The glass slide sat on a heated aluminum plate, which was electrically grounded. See ref 5b. After the films were poled, the heater was turned off and the films were cooled to room temperature with the electric field maintained during the cooling process (typically a 45-min cooling period).

Heating Experiments. The experimental apparatus was specifically designed to provide accurate temperature control while monitoring the second harmonic signal over extended periods of time. The temperature was maintained to within ±2 °C by controlling the power supplied to the electrical heating tape wrapped around the aluminum stage. Details of the experimental apparatus used for the elevated temperature relaxation studies have been previously described.[9]

The films used in the high-temperature relaxation experiments were first aged at ambient room conditions (in air) for about 1-2
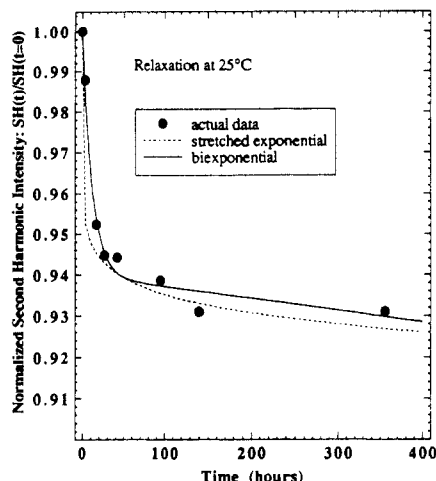
Figure 4. Relaxation of normalized second harmonic signal at 25 °C.

Figure 5. Relaxation of normalized second harmonic signal at 100 °C.

months in the absence of an electric field to ensure that any residual surface charges from the poling process had been dissipated.

After the temperature of the aluminum block had stabilized at the desired temperature, the films were placed on the heating stage. By pressing a thermocouple onto the surface of the film, it was determined that the temperature of the film reached that of the block in about 2 min. In each experiment, the first optical signal was recorded 2 min after the film was placed on the heating stage.

Optical Measurements. Unfocused, parallel polarized light from a Nd:YAG laser (Spectra-Physics GCR-11:1.06-nm wavelength; 10-ns pulse duration; 150–200 mJ per pulse; Q-switched at 10 Hz) was transmitted through the film at the Brewster angle (the angle of incidence was about 60°). The spot size of the laser beam was 0.2-cm² diameter. Each data point represents the average of ten pulses of second harmonic (SH) signal at 532 nm measured by a photomultiplier detector and boxcar averager (Stanford Research SR 280).

The SH intensity was measured with parallel polarized excitation and detection. To ensure both optical and electronic stability during the 40-h elevated-temperature experiments, the following precautions were taken. For optical stability, the SH signal from the reference channel, containing a Y-cut quartz crystal (d_{11} = 0.45 pm/V),[13] and the sample channel were simultaneously monitored in real time. Post electronic processing compensated for laser power fluctuations. For electronic stability, the boxcar data acquisition system was configured to an active baseline subtraction mode to account for electronic DC baseline drifts.

Results

Room Temperature Experiment. At room temperature, after cooling our copolymer films in the poling apparatus and removing the applied poling field, the SH signal decreased about 5% during the first 30 h and about 2% more during the next 320 h, as shown in Figure 4. The optical stability of our polymer is quite good, perhaps enhanced by hydrogen bonding of the amide groups. Relaxation mechanisms will be discussed in more detail later in this paper.

Elevated Temperature Experiments. After at least 30-days aging at room temperature (no applied field), the temperature of poled films was raised in three separate aging experiments to 100, 128, and 141 °C. The temperature was controlled to within ±2° for each experiment. The 38- to 94-h aging behavior of these heated films is shown in Figures 5–7. In all of the elevated-temperature aging experiments, the laser was continuously pulsed (10 Hz) for the first 38–41 h. In the 100 °C aging experiment,
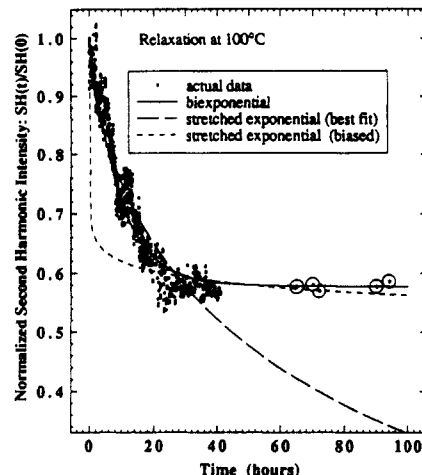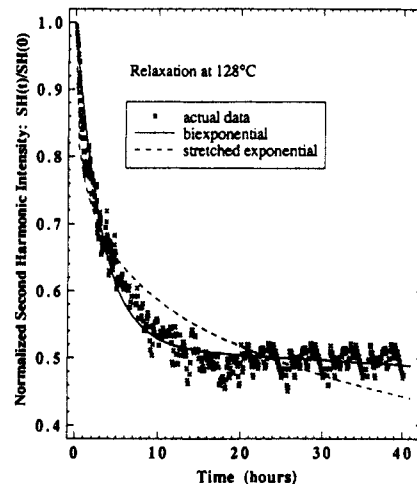

Figure 6. Relaxation of normalized second harmonic signal at 128 °C.
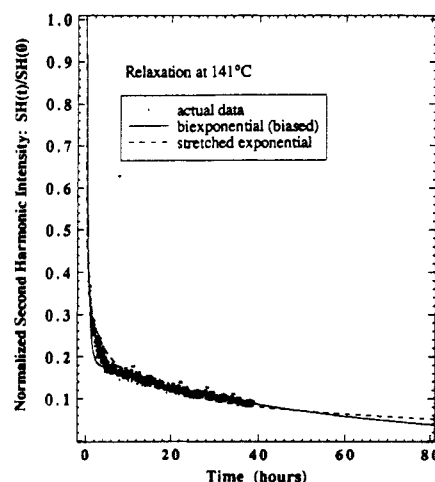
Figure 7. Relaxation of normalized second harmonic signal at 141 °C.

the laser was turned off after 41 h and then turned on intermittently for the final five data points shown in Figure 5; however, the film was maintained continuously at 100 °C for 94 h.

As in the case of the room temperature relaxation measurement, upon heating a polarized film, a relatively rapid initial decay and then a much slower decay of SH signal intensity were observed. To a first approximation, the decay of the normalized SH signal intensity can be

Table I
Constants for Fitting Relaxation Data^a

temp, °C	biexponential, eq 1				stretched exponential, eq 2		
	ϕ	τ_i, h	τ_g, h	$\Sigma^{2\,b}$	τ_α, h	β	$\Sigma^{2\,b}$
25 (Figure 4)	0.06	11.6	33,000	4.8×10^{-5}	10^{10}	0.15	6.5×10^{-4}
100 (Figure 5)	0.42	9.1	20,000	6.8×10^{-1}	83	0.59	1.37×10^0
100 (Figure 5)^c					10^5	0.09	1.19×10^1
128 (Figure 6)	0.48	3.0	740	2.9×10^{-1}	79	0.3	8.9×10^{-1}
141 (Figure 7)	0.77	0.38	34	8.5×10^{-1}	0.70	0.23	6.7×10^{-1}
141 (Figure 7)^d	0.81	0.5	50	1.2×10^0			

^{a} Equations were fit to the data and plotted using Passage. ^{b} Σ^2 = $[(c - o)^2/c]$ where o is the observed datum point and c is the calculated datum point. The residual errors, which are called χ^2 in Passage, are called Σ^2 here to avoid confusion with the second-order NLO coefficient. ^{c} To better fit data at time >40 h with the stretched exponential equation, these coefficients were chosen, as shown in Figure 5 (biased curve). ^{d} To better fit data at time >5 h with the biexponential equation, these coefficients were chosen, as shown in Figure 7 (biased curve).

described by the following biexponential equation:

$$SH(t)/SH(0) = \phi \exp(-t/\tau_i) + (1 - \phi) \exp(-t/\tau_g) \quad (1)$$

The possible physical significance of ϕ and the time constants will be discussed later in this paper.

Another popular and efficient method for empirically fitting relaxation data is the so-called Kohlrausch–Williams–Watts (KWW)[14] or stretched exponential[15] relaxation function:

$$SH(t)/SH(0) = \exp[-(t/\tau_\alpha)^\beta] \quad (2)$$

Curves based on eqs 1 and 2 have been fit through the data points by a least-squares routine. These curves are shown in Figures 4–7. The constants are summarized in Table I. The goodness of fit, over the range of data taken, was somewhat better for the biexponential equation. It is interesting to note for the biexponential equation, the relaxation time constants did not change much with temperature between 25 and 100 °C but decreased considerably in the proximity of T_g. For the stretched exponential equation, there was not a monotonic increase in the exponent β with temperature as one might have expected.

Discussion of Models

First we examine models involving sub-T_g mobility of polymer chain segments. (The possibility of trapped charges diffusing out of the polymer will be discussed later.) The degree of mobility of the sidechains (chromophores) will depend on the locus of the temperature of the experiment relative to the T_g and other solid-state transition temperatures, e.g., the β transition temperature (T_β).[16,8c] Furthermore, at a constant temperature, one must consider the thermal history of the sample, because the slow decrease in specific volume of glasses, called "physical aging",[17] will likely correlate with changes in the optical properties.

Molecular dynamic models involving free volume and the change in free volume distribution in the sample with time are intuitively appealing. Many properties of glassy polymers can be explained by the existence of free volume in the form of discrete microvoids, e.g., non-Fickian diffusion kinetics of small penetrating molecules (the dual mode theory),[18] photoisomerizations and thermal isomerizations of probe molecules,[19] electron spin resonance of probe molecules,[20] and mechanical properties.[21]

Diffusion of defects[22] (or mobility of free volume) is also a key concept for modeling relaxations in glassy polymers. Diffusion of holes and their slow exit through

the surface of a glassy polymer sample was proposed by Curro, Lagasse, and Simha[23] to explain physical aging. However, this model implies that the kinetics of physical aging depends on surface to volume ratio of the macroscopic sample. A study of polystyrene by Braun and Kovaks showed that physical aging does not depend on sample surface to volume ratio.[24] We will come back to this in a moment.

In considering glass-forming liquids, Bendler and Schlesinger predict defect aggregation; i.e., the average hole size increases with time, and the hole mobility decreases with increasing size.[25] However, recent measurements of physical aging using fluorescent probes indicate that "larger pockets of local free volume decrease in number more than the smaller pockets."[19d] At any given temperature, it seems to us that the mobility of large holes would be greater than the mobility of small holes, simply because there are more ways for segments to move into larger holes. If the larger ones move faster, they would exit the sample at a greater rate than the smaller ones. Hence, the average size and hole mobility would decrease with time.

The temporal change in volume is not always a simple asymptotic approach toward an equilibrium value. Other investigators have reported that after heating a sample of aged polycarbonate, the isothermal decrease in modulus lags behind the increase in temperature, goes through a minimum, and then begins to increase (one might say it overshoots then corrects)![26] Kovacs[17a] and Struik[17d] reported similar thermal memory effects in sample volume vs time measurements. Therefore, in considering molecular models, one must take this memory effect into account.

Over 20 years ago, nonuniform distribution of free volume in the glassy state has been proposed to explain physical aging and relaxation behavior in glassy polymers by Simha and Somcynsky,[27] by Paik and Morawetz,[19a] by Yeh,[28] and more recently by Johari.[29] Rivier and Duffy discussed space-filling topology in foams, biological tissues, metallurgical grain-aggregates, and amorphous glasses.[30] We borrow on these ideas and consider a new free volume model involving local heterogeneity, diffusion of holes, and change in the distribution of holes with time.

Proposed Model: Diffusion in Interfaces and Grains (DIG). Since the biexponential equation fits our data fairly well, we wish to consider a molecular picture that has two major relaxation mechanisms and that is consistent with other experimental data on physical aging. Picture an unaged glassy polymer material, one cooled from the "melt" to a temperature well below its glass transition temperature, as having a microscopic grainy texture, one comprised of denser grains whose surfaces form an interconnected, interfacial zone that is less dense, i.e., more defective, softer, and further from equilibrium, than are the grains. As the sample ages, excess free volume (nanometer-sized or smaller holes) from the interfacial zones diffuses out through the sample's surface relatively rapidly. Free volume in the grains diffuses much more slowly into the interfacial zones, where it can then diffuse our more rapidly. The thickness of the interfacial zone is temperature-dependent and may slowly decrease with time but always persists, and for the most part remains interconnected. The holes in grains are smaller, on the average, and less numerous than those in the interfacial zone. The DIG model thus indicates a bimodal distribution of hole sizes.

The DIG model raises the question: can the granular texture be seen by scattering measurements? Is the difference in density between the grains and the interfacial zone great enough to cause scattering of X-rays, electrons,

or neutrons, and what wavelengths will be required to probe the grain size and separation distances?

For many years there has been debate on whether or not small-scale order exists in amorphous glasses and can be detected by scattering measurements.[28,31] Over 10 years ago Uhlmann reported on small-angle X-ray scattering in several amorphous polymer glasses.[32] He discouraged the notion that amorphous polymers are comprised of a large volume percent (e.g., 50%) of nodules having diameters of 50–100 Å. However, he did say the data would accommodate the presence of some nodules, due to the frozen-in thermal fluctuations of polymer configurations. Recent neutron-scattering measurements in calcium silicate glass indicate the presence of medium-range structural order.[33] More definitive neutron-scattering experiments of glassy polymers would appear to be in order. If it can be shown that a local heterogeneous microstructure does not exist, then the DIG model must be abandoned.

Other Models. It is not obvious that holes inside a glassy polymer sample could simply collapse and disappear, because this would require cooperative movement of entire polymer chains or large neighborhoods of chains. However, this might occur when exterior force is applied to the sample such as mechanic deformation or hydrostatic compression. For example, it has been reported that mechanically orienting polycarbonate causes its density and rate of physical aging to increase, compared to an isotropic sample.[20] However, for our experimental data at ambient pressure, and under no external stress, it seems more plausible that movement (diffusion) of holes and their exit through surfaces is the governing mechanism for physical aging.[23]

Holes (or conformational defects) moving down the chain to the chain-end have been proposed.[34] However, there must still be a process responsible for the volumetric contraction of the sample (physical aging). One might consider the existance of two major defect diffusion processes: (1) holes (conformational defects) moving along a polymer backbone and (2) holes jumping from one chain-end to another chain. Physical aging could still be explained by holes escaping from the sample's surface. However, for the case of relaxation of aligned sidechains (dipoles), we would expect that all of the chromophores could relax by means of conformational defects moving along the backbone, and this would not lead to a biexponential SH relaxation.

Interpretation of Second Harmonic Relaxation Data

Relaxation Mechanisms. Spurious relaxation mechanisms, such as the dissipation of surface charges and the evaporation of residual solvent, have been considered. We have baked and aged the samples to minimize these possibilities and believe they are negligible. It is possible that some of the initial SH decay was due to dissipation of trapped space charges injected into the films during the poling process. We did not have instruments to measure space charges; hence we cannot dismiss their consideration. If space charges are present, depending on the size of the charge-carrying species, in the absence of an applied electric field, we believe that the diffusion rate of space charges below T_g would occur no faster than the diffusion of holes in the polymer. Be that as it may, let us examine our data relative to the DIG model.

The DIG Model. Equation 1 can be thought of in terms of a model, where ϕ is the volume fraction of coumarin sidechains in the interfacial zone (considered to be constant for the duration of our experiments), τ_i is the average time
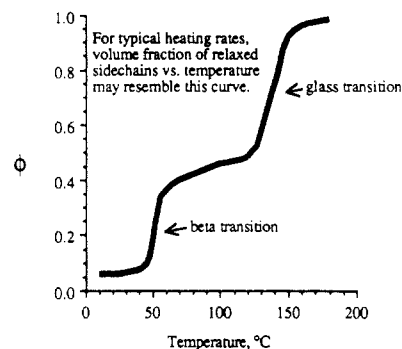

Figure 8. Hypothetical change in ϕ as a function of temperature for sample 1295-6.

constant for diffusion of holes in the interfacial zone, τ_g is the average time constant for diffusion of holes in grains, and t is elapsed time. Both time constants decrease with increasing temperature near the T_g.

As mentioned earlier, if the diffusion coefficient of a hole (at constant temperature) is proportional to the size of the hole (i.e., the larger holes move faster and leave the sample faster than smaller ones), then the average size of the holes will decrease with time. Hence, at constant temperature, the two relaxation time constants in eq 1 would decrease with time. The change is negligible in our experiments but may be important over a period of years.

Unaged Room Temperature Experiment. Immediately after cooling and removing the applied electric field, there was a relatively rapid initial decay and then a much slower decay of SH, as shown in Figure 4. According to the DIG model, the rapid decay could be due to movement of those chromophores that already lie near large, relatively fast moving holes (mostly in the interfacial zone), and the slow part of the decay would be due to those chromophores that must wait until large enough holes diffuse up to them (mostly in the grains). In the DIG model, only after a hole moves up to a sidechain, can the side chain rotate into the hole.

Elevated-Temperature Case. Immediately after heating, the initial rapid decay may be a function of the rate of volumetric thermal expansion. In our heating experiments, the initial part of the SH decay, according to the DIG model, is due to free volume that flowed into the sample from the exterior surfaces and was channeled through the interconnected interfacial zone. Free volume (holes) can also diffuse into the grains, but this occurs much more slowly. The interfacial zone increases in thickness and in volume due to the surface regions of the grains melting and transforming into interfacial zone material. This also implies that entropic changes lag enthalpic changes in glassy polymers.

The initial large decrease in SH in our heating experiments could be related to the memory effect, i.e., a local overshoot in the increase of free volume upon heating. In the DIG model, it would be the interfacial zone that initially becomes overextended and then shrinks slightly as the grains become more involved by voids diffusion into them. Perhaps this transient, heterogeneous distribution of excess free volume and heat capacity could be detected by solid-state NMR.

β-Transition. Way below the T_β, complete relaxation of all of the chromophores may essentially never occur. Although we do not have SH relaxation data near T_β (52 °C), upon heating the sample from room temperature, it is tempting to speculate that ϕ may increase rather rapidly near T_β, then plateau until near the T_g, and then increase rapidly to 1.0 once past the T_g. Figure 8 schematically

shows how ϕ might increase as a function of temperature for our polymer. However, note that τ_i did not change much between 25 and 100 °C (see Table I). This would indicate that the number of holes and not the mobility of the holes increases upon passing through T_β. One explanation for this behavior is that T_β represents a temperature at which some grain material is converted into interfacial zone material, whereas the hole mobilities in each of the two zones remain fairly constant until the T_g is reached. This interpretation is in harmony with conclusions drawn from observations of the sub-T_g mechanical relaxations in poly(methyl methacrylate), that the increase in height of the β relaxation peak with increasing temperature is due to the *number* of chain segments that undergo thermally activated motions.[35]

Molecular Weight. This study has not addressed the effect of polymer molecular weight (chain length) on relaxation behavior. The size of the grains formed as the polymer is cooled from above T_g, and the ratio of the amount of grain to interfacial zone material, may be dependent on the molecular weight of the polymer chain. The amount of grain material that is converted into interfacial material at a given temperature (and the rate of that process) could be a function of the polymer molecular weight.

Further Considerations. It should be noted that our sample has a huge surface to volume ratio (10^6 m^2/m^3). The cast polymer film is undoubtedly experiencing a compressive force caused by the the the mismatch in thermal expansion coefficients between the polymer film and the glass substrate to which it tightly adheres. This force may also affect the rate of physical aging.

Future Studies

Nonlinear optical polymers having glass transitions near 100 °C, in which the sidechains are smaller than our coumarin group, relax fairly rapidly even at room temperature.[36] It would be informative to measure SH relaxation by using a series of side-chain probes of different sizes. In the DIG model, the time constants will be a function of the ratio of the average size of holes to the actual size of the chromophore in each of the two regions (and the concentration of holes and chromophores in the two regions).

The way is clear for chemists to make more stable nonlinear optical films. Using larger chromophores,[37] incorporating the chromophores in the polymer backbone (main-chain chromophores),[38] and/or cross-linking the polymer matrix[39] will increase the long-term orientational stability of the chromophore. However, if the poling temperature is too high, thermal fluctuations (kT) will fight against the aligning torque of the poling field. Hence, new processing techniques must be developed.

Conclusions

Second harmonic signal (SH) decay in poled glassy polymers is a useful technique for investigating polymer chain dynamics near and below the T_g. A biexponential model fits at least the first 100 h of SH relaxation data at elevated temperatures in our poled side-chain polymer and gives a slightly better fit to the data than does a stretched exponential model. A model that considers diffusion of holes in a locally heterogeneous matrix successfully accounts for the relaxation data and known physical aging effects, including the lack of dependence on the sample's surface to volume ratio. Samples should be aged 10 or 20 deg below the T_g for 5-10 h to allow some of the nonequilibrium free volume to vacate the sample

in order to stabilize the nonlinear optical properties. More work is needed on measuring trapped space charges in poled glassy polymer films and their affect on the long-term stability of polar order.

References and Notes

(1) (a) Garito, A. F.; Wong, K. Y.; Zamani-Khamiri, O. In *Nonlinear Optical and Electroactive Polymers*; Prasad, P. N., Ulrich, D. R., Eds.; Plenum: New York, 1987. (b) *Nonlinear Optical Properties of Organic Molecules and Polymeric Materials*; Chemla, D. S., Zyss, J., Eds.; Academic: New York, 1987; Vol. 1. (c) Prasad, P. N.; Williams, D. J. *Introduction to Nonlinear Optical Effects in Molecules and Polymers*; John Wiley & Sons: New York, 1991.

(2) Cross, G. H.; Donaldson, A.; Gymer, R. W.; Mann, S.; Parsons, N. J.; Haas, D. R.; Man, H. T.; Yoon, H. N. *Proc. SPIE* **1989**, *1177*, 79.

(3) (a) McFarland, M. J.; Wong, K. K.; Wu, C.; Nahata, A.; Horn, K. A.; Yardley, J. T. *Proc. of the SPIE* **1988**, *993*, 26. (b) Kaczmarski, P.; Van de Capelle, J.-P.; Lagasse, P. E.; Meynart, R. *IEEE Proc.* **1989**, *136 Pt. J*, 152.

(4) Eldering, C. A.; Kowel, S. T.; Brinkley, P.; Matloff, N.; Schubert, T.; Gosula, R. *Proc. SPIE* **1989**, *1151*, 72.

(5) (a) Singer, K. D.; Kuzyk, M. G.; Holland, W. R.; Sohn, J. E.; Lalama, S. L.; Comizzoli, R. B.; Katz, H. E.; Schilling, M. L. *Appl. Phys. Lett.* **1988**, *53*, 1800. (b) Mortazavi, M. A.; Knoesen, A.; Kowel, S. T.; Higgins, B. G.; Dienes, A. *J. Opt. Soc. Am. B* **1989**, *6*, 733. (c) van der Vorst, C. P. J. M.; Picken, S. J. *J. Opt. Soc. Am. B* **1990**, *7*, 320.

(6) Shen, Y. R. *The Principals of Nonlinear Optics*; John Wiley & Sons: New York, 1984.

(7) (a) Boyd, G. T. *Thin Solid Films* **1987**, *152*, 295. (b) Hampsch, H. L.; Yang, J.; Wong, G. K.; Torkelson, J. M. *Polym. Commun.* **1989**, *30*, 40. (c) Lindsay, G.; Hoover, J.; Knoesen, A.; Mortazavi, M.; Kowel, S. *Am. Chem. Soc., Div. Polym. Chem., Polym. Prepr.* **1990**, *31*, 255.

(8) (a) Hampsch, H. L.; Yang, J.; Wong, G. K. Torkelson, J. M. *Macromolecules* **1988**, *21*, 526. (b) Hubbard, M. A.; Marks, T. J.; Yang, J.; Wong, G. K. *Chem. Mater.* **1989**, *1*, 167. (c) Meyrueix, R.; Mignani, G. *SPIE Proc.* **1989**, *1127*, 160. (d) Hampsch, H. L.; Torkelson, J. M.; Bethke, S. J.; Grubb, S. G. *J. Appl. Phys.* **1990**, *67*, 1037. (e) Hampsch, H. L.; Yang, J.; Wong, G. K.; Torkelson, J. M. *Macromolecules* **1990**, *23*, 3640, 3648. (f) Singer, K. D.; King, L. A. *J. Appl. Phys.* **1991**, *70*, 3251.

(9) Mortazavi, M. A.; Knoesen, A.; Kowel, S. T.; Henry, R. A.; Hoover, J. M.; Kubin, R. F.; Lindsay, G. A. *Appl. Phys. B* **1991**, *53*, 287.

(10) (a) Hayden, L. M.; Sauter, G. F.; Ore, F. R.; Pasillas, P. L.; Hoover, J. M.; Lindsay, G. A.; Henry, R. A. *J. Appl. Phys.* **1990**, *68*, 456. (b) Henry, R. A.; Hoover, J. M.; Knoesen, A.; Kowel, S. T.; Lindsay, G. A.; Mortazavi, M. A. *Mat. Res. Soc. Symp. Proc.* **1990**, *173*, 601. (c) Henry, R. A.; Hoover, J. M.; Lindsay, G. A. *Navy Case No. 72263, U.S. Patent Appl.* Serial 680.717, 1991.

(11) Data provided by: Kubin, R. F. using MOPAC 5.0 at Michelson Laboratory, China Lake, CA.

(12) Lantman, C. W.; Tassin, J. F.; Sergot, P.; Monnerie, L. *Macromolecules* **1989**, *22*, 483.

(13) Kurtz, S. K.; Jerphagnon, J.; Choy, M. M. *Landolt–Bornstein Numerical Data and Functional Relationships in Science and Technology*; Springer: New York, 1979; Vol. 11, p 671.

(14) (a) Kohlrausch, R. *Pogg. Ann. Phys.* **1854**, *1*, 179. (b) Williams, G.; Watts, D. C. *Trans. Faraday Soc.* **1970**, *66*, 80. (c) Torell, L. M.; Boerjesson, L.; Elmroth, M. *J. Phys., Condens. Matter* **1990**, *2*, SA207.

(15) (a) Li, K. L.; Ingefeld, P. T.; Jones, A. A.; Bender, J. T.; English, A. D. *Macromolecules* **1988**, *21*, 2940. (b) Scher, H.; Schlesinger, M. F.; Bendler, J. T. *Phys. Today* **1991**, *Jan*.

(16) Adam, G.; Gibbs, J. *J. Phys. Chem.* **1965**, *43*, 139.

(17) (a) Kovaks, A. J. *Fortschr. Hochpolym.-Forsch.* **1962**, *3*, 394. (b) Kovaks, A. J.; et al. *J. Polym. Sci., Phys. Ed.* **1979**, *17*, 765.

(c) *Ibid.* **1979**, *17*, 2031. (d) Struik, L. C. E. *Physical Aging in Amorphous Polymers and other* Materials; Elsevier: Amsterdam, 1978. (e) *Structure and Mobility in Molecular and Atomic Glasses*; O'Reilly, J. M., Goldstein, M., Ed.; Annals of the New York Academy of Sciences; New York, 1981; Vol. 371.

(18) (a) Petropoulos, J. H. *J. Polym. Sci., Polym. Phys. Ed.* **1970**, *8*, 1797. (b) Koros, W. J.; Paul, D. R. *J. Polym. Sci. Polym. Phys. Ed.* **1978**, *16*, 1947. (c) Stewart, H. B.; Hopfenberg, M. E.; Koros, W. J. *J. Appl. Polym. Sci.* **1989**, *38*, 1111. (d) Petropoulos, J. H. *J. Polym. Sci.: Part B: Polym. Phys.* **1989**, *27*, 603. (e) Horas, J. A.; Reyes, E. R.; Magnin, J. E. *J. Polym. Sci: Part B: Phys. Ed.* **1991**, *28*, 1153.

(19) (a) Paik, C. S.; Morawetz, H. *Macromolecules* **1972**, *5* (2), 177. (b) Victor, J. G.; Torkelson, J. M. *Macromolecules* **1987**, *20*, 2954. (c) Meyer, E. F.; Jamieson, A. M.; Simha, R.; Palmen, J. H. M.; Booij, H. C.; Maurer, F. H. J. *Polymer* **1990**, *31*, 243. (d) Royal, J. S.; Victor, J. G.; Torkelson, J. *Macromolecules* **1992**, *25*, 729.

(20) Bartos, J.; Mueller, J.; Wendorff, J. H. *Polymer* **1990**, *31*, 1678.

(21) Donth, E.; Michler, G. H. *Colloid Polym. Sci.* **1989**, *267*, 557.

(22) Glarum, S. H. *J. Chem. Phys.* **1960**, *33*, 639.

(23) Curro, J. G.; Lagasse, R. R.; Simha, R. *Macromolecules* **1982**, *15*, 1621.

(24) Braun, G.; Kovaks, A. J. *Phys. Chem. Glasses* **1963**, *4*, 152.

(25) Bendler, J. T.; Schlesinger, M. F. *J. Stat. Phys.* **1991**, *53*, 531.

(26) Haidar, B.; Smith, T. *Macromolecules* **1990**, *23*, 3712.

(27) Simha, R.; Somcynsky, T. *Macromolecules* **1969**, *2*, 342.

(28) Yeh, G. S. Y. *J. Macromol. Sci., Phys.* **1972**, *B6*, 451.

(29) (a) Johari, G. P. *J. Physique* **1985**, *46*, C8-567. (b) Johari, G. P. In *Phase Transitions*; Gordon and Breach: United Kingdom, 1985, Vol. 5, pp 277–300.

(30) (a) Rivier, N. *Physica* **1986**, *23D*, 129. (b) Rivier, N.; Duffy, D. M. *J. Physique* **1982**, *43*, 293. (c) Rivier, N. *Helv. Phys. Acta* **1983**, *56*, 307.

(31) Schubach, H. R.; Nagy, E.; Heise, B. *Colloid Polym.* **1981**, *259*, 789.

(32) Uhlman, D. R. *Faraday Discuss., R. Soc. Chem.* **1979**, *68*, 87.

(33) Gaskell, P. H.; Eckersley, M. C.; Barnes, A. C.; Chieux, P. *Nature* **1991**, *350*, 675.

(34) (a) Bendler, J. T.; Schlesinger, M. F. *J. Mol. Liq.* **1987**, *36*, 37. (b) Legrand, D. G.; Olszewski, W. V.; Bendler, J. T. *J. Polym. Sci., Polym. Phys. Ed.* **1987**, *25*, 1149.

(35) Muzeau, E.; Perez, J.; Johari, G. P. *Macromolecules* **1991**, *24*, 4713.

(36) (a) Eich, M.; Sen, A.; Looser, H.; Bjorklung, G. C.; Swalen, J. D.; Twieg, R.; Yoon, D. Y. *J. Appl. Phys.* **1989**, *66* (6), 2559. (b) Page, R. H.; Jurich, M. C.; Rech, B.; Sen, A.; Twieg, R. J.; Swalen, J.; Bjorklund, G. C.; Wilson, C. G. *J. Opt. Soc. Am. B.* **1990**, *7*, 1239. (c) Ye, C.; Minami, N.; Marks, T. J.; Yang, J.; Wong, G. K. *Macromolecules* **1991**, *21*, 2899. (d) Eich, M.; Sen, A.; Looser, H.; Yoon, D. Y.; Bjorklund, G. C.; Twieg, R.; Swalen, J. D. *Proc. SPIE* **1991**, *971*, 128. (e) Park, J.; Marks, T. J.; Yang, J.; Wong, G. K. *Chem. Mater.* **1991**, *2*, 229.

(37) Katz, H. E.; Schilling, M. L.; Fang, T.; Holland, W. R.; King, L.; Gordon, H. *Macromolecules* **1990**, *24*, 1201.

(38) (a) Fuso, F.; Padia, A. B.; Hall, H. K., Jr. *Macromolecules* **1991**, *24*, 1710. (b) Stenger-Smith, J. D.; Fischer, J. W.; Henry, R. A.; Hoover, J. M.; Nadler, M. P.; Nissan, R. A.; Lindsay, G. A. *J. Polym. Sci., Part A: Polym. Chem.* **1991**, *29*, 1623. (c) Koehler, W.; Robello, D. R.; Willand, C. S.; and Williams, D. J. *Macromolecules* **1991**, *24*, 4589.

(39) (a) Eich, M.; Reck, B.; Yoon, D. Y.; Wilson, C. G.; Bjorklund, G. C. *J. Appl. Phys.* **1989**, *66* (7), 3241. (b) Park, J.; Marks, T. J.; Yang, J.; Wong, G. K. *Chem. Mater.* **1990**, *2* (3), 229. (c) Jungbauer, D.; Reck, B.; Twieg, R.; Yoon, D. Y.; Willson, C. G.; Swalen, J. D. *Appl. Phys. Lett.* **1990**, *56* (26), 2610. (d) Mandal, B. K.; Kumar, J.; Huang, J.-C.; Tripathy, S. *Makromol. Chem., Rapid Commun.* **1991**, *12*, 63.